

## PATTERNED LASER CRYSTALLIZATION OF a-Si

B. Polyakov<sup>1\*</sup>, G. Marcins<sup>1</sup>, M. Chubarov<sup>1</sup>,  
A. Kuzmin<sup>1</sup>, V. Klykov<sup>2</sup> and I. Tale<sup>1</sup>

<sup>1</sup>Institute of Solid State Physics, University of Latvia,  
8 Kengaraga Str., Riga, LV-1063, LATVIA

<sup>2</sup>Sidrabe Inc.,  
17 Krustpils Str., Riga, LV-1073, LATVIA

\*e-mail: boris.polyakov@cfi.lu.lv

Thin films of amorphous Si on glass were crystallized by pulsed nano- and picosecond lasers. Two methods for creating the desired patterns of crystallized regions were used. In the former, the pattern is produced by a focused laser beam, and in the latter it is made using a prefabricated mask. The electric conductivity of crystallized films increases by more than 4 orders of magnitude in comparison with untreated amorphous films.

## 1. INTRODUCTION

Recently, transformation of amorphous Si (a-Si) deposited on a low melting temperature substrate (glass, plastic) into polycrystalline silicon (p-Si) has become rather a popular topic [1]. Polycrystalline silicon has superior electronic properties in comparison with a-Si, and it is viewed as a very attractive material for thin-film electronic devices, such as field effect transistors (FET) and high-efficiency low-cost thin film solar cells [2, 3, 4]. Surface modifications that attend laser crystallization may be useful in some applications, e.g. electron field emission [5]. Common approaches employed to crystallize a-Si are solid phase crystallization (SPC) [6], metal-induced crystallization (MIC) [7] and electric-field enhanced metal-induced crystallization (EF-MIC) [8, 9]. The SPC is based on isothermal annealing of a-Si at a temperature of about 600°C. The second approach (MIC) is based on the effect according to which definite metals being in contact with amorphous silicon induce transformation from the amorphous to the crystalline phase at the temperatures well below the eutectic temperature of a metal-silicon system. The electric field (EF-MIC approach) increases significantly the rate of metal-induced crystallization. However, the most attractive method of producing p-Si is based on the use of laser crystallization (LC) process [10, 11]. Using the interference of split laser beams, a-Si films may be crystallized into parallel lines [12]. In order to perform laser crystallization of a-Si, a nano- or picosecond UV laser pulses strongly absorbed in material are usually used, so the transformation from amorphous to crystalline silicon occurs by local melting the material for a very short time. It is also possible to achieve different crystallization regimes by varying the laser intensity thus changing electrical and optical properties of the resultant p-Si film. Here we report two methods that could be employed to create p-Si crystallized regions of a desired arbitrary pattern.

## 2. EXPERIMENTAL

In our experiments we used Al-doped samples of a-Si thin film (160 nm) deposited by rotational magnetron sputtering on a glass substrate. The film was sputtered from a Si–Al target (10%) in the Ar atmosphere at  $2 \cdot 10^{-3}$  torr. The magnetron power was 10 kW, the deposition rate – 50 nm/min, and the target-to-substrate distance – 140 mm.

The laser treatment with a focused laser beam was performed using a high repetition rate UV (355 nm) nanosecond laser Techno35 and a picosecond laser PL10100 (*Expla*). To crystallize the whole sample of a-Si film we employed an unfocused Nd:YAG laser (SL-312, *Ekspla*), third harmonic (355 nm), pulse duration 135 ps, and 10 Hz repetition rate. For the mask we took the copper grid of a transmission electron microscope (TEM), 600 mesh (*Agar Scientific*).

The surface topography was measured by CP-II AFM (*Veeco*) using silicon tips (DP15, *Mikromasch*). The optical images were taken by Eclipse L150 (*Nikon*) optical microscope. Raman scattering spectra were measured on a 3D scanning confocal microscope with a Nanofinder-S (Solar-TII) spectrometer [11]. A HeCd laser (441.6 nm, 50 mW CW power) was used as the light source. The measurements were performed through a Nikon CF Plan Apo 100x (NA=0.95) optical objective. The Raman spectra were recorded using a 600 grooves/mm diffraction grating ( $\sim 3\text{--}4 \text{ cm}^{-1}$  resolution), a monochromator (520 mm focal length) and an edge filter to eliminate the laser's elastic component.

Aluminium contacts were deposited on the samples by thermal evaporation to measure electrical parameters of the films. The current-voltage curves were measured using a function generator (33220A, Agilent), a multimeter 2000 and a 6485 picoammeter (Kethley).

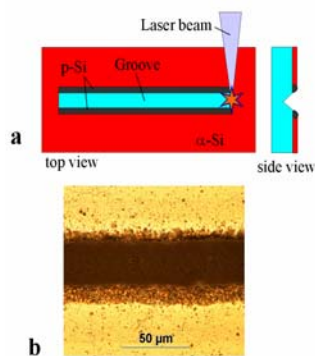


*Fig. 1.* Groove cutting by laser (a). Optical microscope image (b). Formation of electrodes for measuring stripe resistance (c).

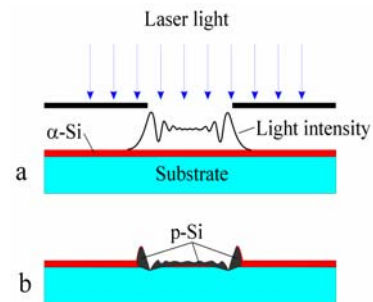


*Fig. 2.* Laser crystallization through mask (a). Sample after crystallization (b).

## 3. RESULTS

We therefore used two treatment methods, without and with a mask, to crystallize a-Si thin film on a glass substrate by laser irradiation. In the first treatment method, a number of parallel lines were drawn on the film (see Fig. 1)

using a focused (spot size 5  $\mu\text{m}$ ) pulsed (nanosecond and picosecond) laser beam (actually, any arbitrary 2D shape may be drawn using such a laser setup). Narrow grooves were formed under the laser path in a glass substrate and in the a-Si thin film. Stripe of the same size were also produced by a diamond tip to compare electrical properties of the stripes. Metallic electrodes (Al) were deposited by thermal evaporation on the stripes of a-Si to measure their electrical resistance (Fig. 1c). We have found that the resistance of a stripe produced by a diamond tip is significantly higher than that of a laser-made stripe. This result can be explained by laser-induced crystallization of a-Si film, i.e. by formation of a narrow region of polycrystalline silicon (p-Si) along the groove (Fig. 1a). The calculated resistance of a-Si stripe (10 mm long and 1 mm wide, formed by diamond scratching) is about 75 M $\Omega$ , whereas that for picosecond and nanosecond laser cut stripes is 14 M $\Omega$  and 4 M $\Omega$ , respectively. The resistance of p-Si region produced by a nanosecond laser is lower than that of such produced by a picosecond laser, because more energy is supplied by the former laser to the neighbourhood of the groove in a-Si region during the laser cutting. Thus crystallized region is only few microns wide, so we call it a microwire. The amorphous silicon strip and two crystallized regions at its both sides are equivalent to three resistors connected in parallel. Keeping this in mind, we calculated the microwire resistance and obtained 34 M $\Omega$  and 8.4 M $\Omega$  for the picosecond and nanosecond lasers, respectively. Thus we could form a pair of p-Si microwires drawing lines by laser on the a-Si thin film.

The influence of laser crystallization on a-Si electroconductive properties was studied using a 355 nm pulsed laser (135 ps). The 1 $\times$ 1 cm<sup>2</sup> samples cut from the same a-Si coated glass plate were crystallized by laser light of intensity 160 mJ/cm<sup>2</sup> for 60 s. The Hall measurements using the van-der-Pauw method were performed on as-deposited and laser-crystallized samples: the carrier concentration was 1.93 $\cdot$ 10<sup>17</sup> and 2.24 $\cdot$ 10<sup>20</sup> cm<sup>-3</sup> and the carrier mobility was 0.212 and 4.82 cm<sup>2</sup>/Vs, respectively. Thus, laser crystallization significantly improves a-Si film conductivity through the dopant activation and increased carrier mobility. A large portion of dopant atoms are inactive in as-prepared a-Si film due to improper position in the a-Si network. The energy supplied by the absorbed laser light during crystallization helps dopant atoms to form bonds with Si atoms and to embed into the Si lattice in a proper position. After that the dopant atoms become electrically active. The higher mobility of charge carriers in p-Si, compared with a-Si, is due to its ordered structure.

In the second treatment method, we illuminated a-Si thin film on a glass sample by 355 nm pulsed laser (135 ps) through a contact mask, fluence  $\sim$  200 mJ/cm<sup>2</sup> (Fig. 2). As the mask, a commercial TEM grid with 22 $\times$ 22  $\mu\text{m}^2$  square windows was used. Due to diffraction phenomena, the laser light has maximum intensity along the edge of a mask window (Fig. 2a). The morphology of sample surface after laser crystallization was measured by a tapping-mode AFM (Fig. 3). The measurements have shown that mass transfer occurs along the edge of a treated region. It is interesting to note that the groove depth was about 200 nm, which is greater than the thickness of a-Si layer. However, it is not clear if such phenomena could occur on a substrate with a high melting temperature (e.g. Al<sub>2</sub>O<sub>3</sub> instead of glass).

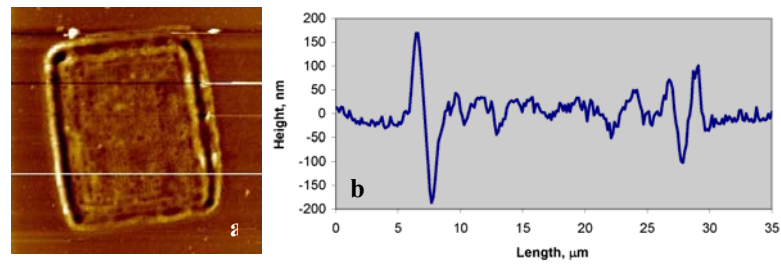


Fig. 3. AFM image of crystallized region,  $35 \times 35 \mu\text{m}$ . The white line marks cross-section (a). Corresponding cross-section (b).

To prove the crystalline nature of the laser-treated region we have performed the micro-Raman measurements using a confocal optical microscope. It is known [13, 14] that Raman scattering spectra may be used to estimate the fractions of crystalline and amorphous phases in Si thin films after laser crystallization. The broad Raman band centred at  $480 \text{ cm}^{-1}$  (Fig. 4) is associated with amorphous Si [13]. The Brillouin zone centre optical mode observed in the Raman spectrum of monocrystalline Si at  $\sim 520 \text{ cm}^{-1}$  shifts to  $517 \text{ cm}^{-1}$  and broadens in polycrystalline Si [14]. Several Raman spectra were measured in untreated and laser-crystallized regions. The results indicate that the untreated region of the film is not fully amorphous but contains some fraction of nanocrystals. Note that in our spectra the scattering peaks at  $480 \text{ cm}^{-1}$  and  $517 \text{ cm}^{-1}$  are mixed up (Fig. 4c). The Raman signal at  $517 \text{ cm}^{-1}$  is strongly enhanced in the laser-crystallized region, which evidences that the process of laser crystallization was successful. To study the distribution of crystalline phase across the film, a spatial map of Raman signal at a selected ( $517 \text{ cm}^{-1}$ ) wavelength (spectral image) was obtained simultaneously with the confocal image using a Nanofinder-S confocal microscope. The results show that the Raman signal corresponding to crystallized Si originates mostly from the laser-treated regions (compare Figs. 4a and b).

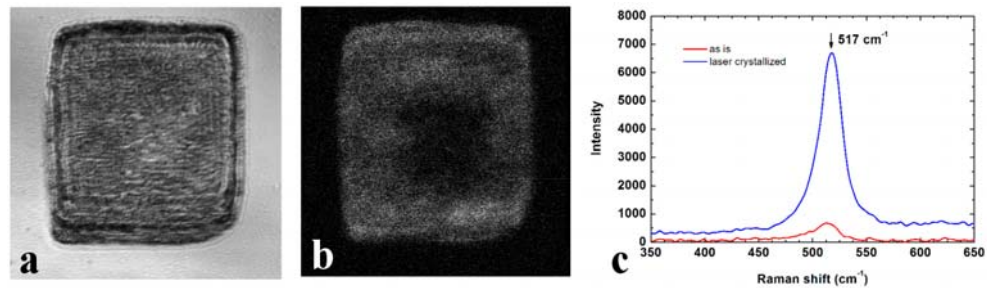


Fig. 4. Confocal optical microscope image of laser-crystallized square region, image size  $38 \times 38 \mu\text{m}$  (a). Spectral image taken simultaneously with (a) at the maximum of the  $517 \text{ cm}^{-1}$  Raman band (b). Raman spectra taken in untreated (outside the square in (a)) and laser-crystallized (inside the square in (a)) regions (c).

#### 4. CONCLUSIONS

It is shown that thin films of amorphous silicon (a-Si) can easily be crystallized by nano- and picosecond lasers. Desired patterns can be drawn by a

laser on a-Si sample surface to obtain crystallized paths of high conductivity. The conductivity of laser-crystallized Si film (at 160 mJ/cm<sup>2</sup>) increases more than 4 orders of magnitude in comparison with untreated amorphous films, mainly due to dopant activation. Desired patterns of crystallized Si can also be formed by laser crystallization through a mask. In this case, mass transfer of melted Si along the edge of a mask window was observed. The effect of the underlying substrate needs to be specified.

#### ACKNOWLEDGMENTS

*The authors are grateful to Dr. J. Maniks and A. Tokmakov for help and assistance. Special thanks to Dr. G.Raciukaitis and G.Kudaba from Expla company.*

#### REFERENCES

1. Yi Ch., Rhee, S., Ju, J., Yim, S., & Min, H. (2001). *J. Mater. Sci. Mater. Electron.*, 12, 697.
2. Brotherton, S., Ayres, J., Edwards, M., Fisher, C., Glaister, C., Gowers, J., McCulloch, D., & Trainor, M. (1999). *Thin Solid Films*, 337, 188.
3. Kim, Y., Hwang, C., Song, Y., Chung, C., Ko, Y., Sohn, C., Kim, B., & Lee, J. (2003). *Thin Solid Films*, 440, 169.
4. Bergmann, R. (1999) *Appl. Phys. A*, 69, 187.
5. O'Neill, K., Shaikh, M., Lyttle, G., Anthony, S., Fan, Y., Persheyev, S., & Rose, M. (2006). *Thin Solid Films*, 501, 310.
6. Yamauchi, N., & Reif, R. (1994) *J. Appl. Phys.*, 75, 3235.
7. Herd, S., Chaudhari, P., & Brodsky, M. (1972). *J. Non-Cryst. Solid*, 7, 309.
8. Yoon, S., Park, S., Kim, K., & Jang, J. (2001). *Thin Solid Films*, 383, 34.
9. Rezek, B., Sipek, E., Ledinsky, M., Krejza, P., Stuchlik, J., Fejfar, A., & Kocka, J. (2008). *J. Non-Crystal. Solids*, 354, 2305.
10. Poate, J. & Mayer, J. (1982). *Laser Annealing of Semiconductors*. New York: Academic Press.
11. Kuzmin, A., Kalendarev, R., Kursitis, A., & Purans, J. (2006). *Latv. J. Phys. Tech. Sci.*, (2) 66.
12. Rezek, B., Nebel, C., & Stutzmann, M. (2002). *J. Appl. Phys.*, 91, 7 4220.
13. Viera, G., Huet, S., & Boufendi, L. (2001) *J. Appl. Phys.*, 91, 8 4175.
14. Lengsfeld P. (2001) Successive laser crystallization of doped and undoped a-Si:H. *PhD thesis* (Berlin).

#### AMORFA SILĪCIJA (a-Si) STRUKTURĒTA LĀZERKRISTALIZĒŠANA

B. Poļakovs, G. Mārciņš, M. Čubarovs, A. Kuzmins, V. Klikovs, I. Tāle

#### K o p s a v i l k u m s

Amorfa silīcija plānās kārtiņas uz stikla tika kristalizētas ar impulsu nano-sekunžu un piko-sekunžu lāzeriem. Izmantotas divas metodes polikristāliska silīcija raksta iegūšanai. Pirmajā metodē raksts iegūts, pārvietojot fokusētu lāzera staru, bet otrajā metodē rakstu iegūst, paraugu apstarojot caur iepriekš izgatavotu masku. Iegūtā polikristāliskā silīcija vadāmība pieaug vairāk kā par 4 kārtām, salīdzinot ar neapstrādātu paraugu.